

AD-A120 526

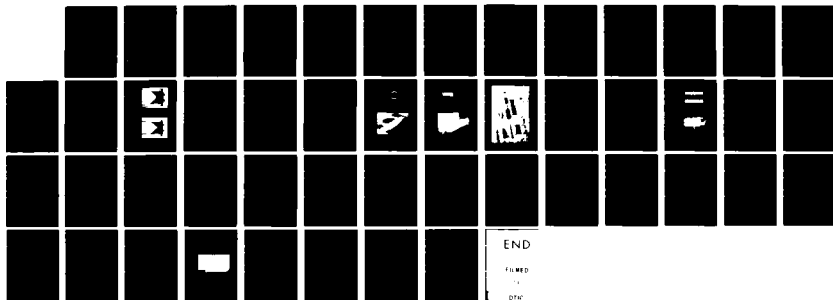
HIGH POWER PULSED PLASMA MHD EXPERIMENTS(U) ARTEC
ASSOCIATES INC HAYWARD CA D W BAUM ET AL. 30 SEP 82
AR-165 N00014-81-C-0045

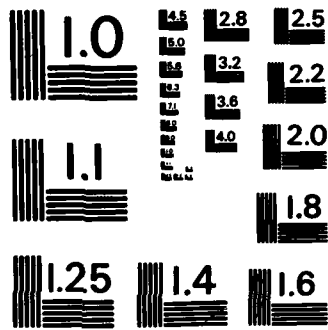
1/1

UNCLASSIFIED

F/G 20/9

NL



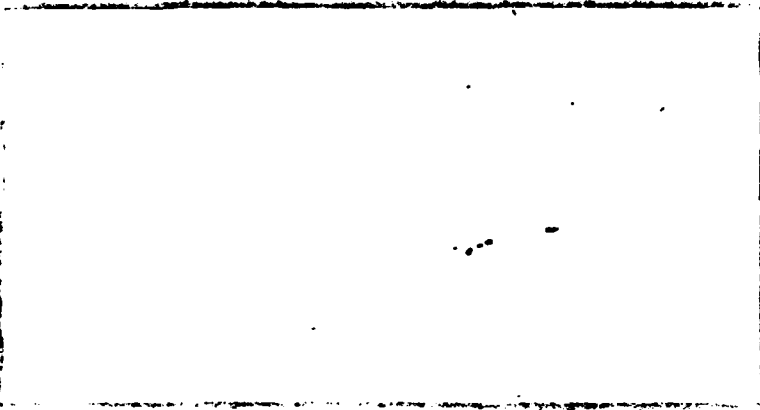


MICROCOPY RESOLUTION TEST CHART
NATIONAL BUREAU OF STANDARDS-1963-A

LEVEL II

12

AD A120526



This document has been approved for public release and sale; its distribution is unlimited.

DTIC
S OCT 19 1982 J
E

DIC FILE COPY

ARTEC  ASSOCIATES·INC

82_10 19 041

REPORT DOCUMENTATION PAGE		READ INSTRUCTIONS BEFORE COMPLETING FORM
1. REPORT NUMBER AR-165	2. GOVT ACCESSION NO. AD A120 526	3. RECIPIENT'S CATALOG NUMBER
4. TITLE (and Subtitle) High Power Pulsed Plasma MHD Experiments		5. TYPE OF REPORT & PERIOD COVERED Annual Report 81Jan01 to 82Sep30
		6. PERFORMING ORG. REPORT NUMBER
7. AUTHOR(s) D.W. Baum, S.P. Gill, W.L. Shimmin, J.D. Watson		8. CONTRACT OR GRANT NUMBER(s) N00014-81-C-0045
9. PERFORMING ORGANIZATION NAME AND ADDRESS Artec Associates Incorporated 26046 Eden Landing Road Hayward, California 94545		10. PROGRAM ELEMENT, PROJECT, TASK AREA & WORK UNIT NUMBERS
11. CONTROLLING OFFICE NAME AND ADDRESS Department of the Navy Office of Naval Research Arlington, Virginia 22217		12. REPORT DATE 82 Sep 30
		13. NUMBER OF PAGES 47
14. MONITORING AGENCY NAME & ADDRESS (if different from Controlling Office)		15. SECURITY CLASS. (of this report) Unclassified
		15a. DECLASSIFICATION/DOWNGRADING SCHEDULE
16. DISTRIBUTION STATEMENT (of this Report) Unclassified; Unlimited		
17. DISTRIBUTION STATEMENT (of the abstract entered in Block 20, if different from Report)		
18. SUPPLEMENTARY NOTES		
19. KEY WORDS (Continue on reverse side if necessary and identify by block number) Pulsed Plasma MHD, Magnetohydrodynamics, Pulsed Power, Prime Power, Dense Nonideal Plasmas		
20. ABSTRACT (Continue on reverse side if necessary and identify by block number) Results of high power pulsed plasma MHD experiments are reported. An explosively driven plasma source is used to drive a Faraday mode MHD generator with an externally applied B-field of several tesla. The highest power achieved was 6 gigawatts in a 140 kJ electrical pulse delivered to a resistive load. The experimentally observed scaling relationships of power with applied B-field and electrode area are also presented.		

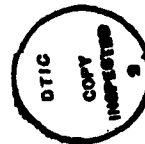
High Power Pulsed Plasma MHD
Experiments

Annual Report AR-165

30 September 1982
Final Report for Period 1 January 1981 to 30 September 1982

Sponsored by: Department of the Navy
Office of Naval Research
800 North Quincy Street
Arlington, Virginia 22217

Prepared by: D.W. Baum, S.P. Gill, W.L. Shimmin and
J.D. Watson
Artec Associates Incorporated
26046 Eden Landing Road
Hayward, California 94545
Telephone: 415/785-8080



Accession For	
NTIS GRA&I	<input checked="" type="checkbox"/>
DTIC TAB	<input type="checkbox"/>
Unannounced	<input type="checkbox"/>
Justification	
By	
Distribution/	
Availability Codes	
Dist	Avail and/or Special
A	

Table of Contents

	Page
Acknowledgement	5
1.0 Introduction	6
2.0 Pulsed Plasma MHD	8
2.1 Plasma States	8
2.2 Plasma Source	11
2.3 Faraday Mode MHD Generator	13
2.4 Experimental Arrangement and Diagnostics	17
3.0 High Power MHD Experimental Results	25
3.1 Plasma Flow Conditions	25
3.2 MHD Generator Performance	31
3.3 Scaling Relationships	37
3.4 Electric Circuit-Plasma Flow Interactions	40
3.5 Effect of MHD Channel Diameter	44
4.0 Conclusions	45
References	47

List of Figures

	Page
Figure 1. Argon Plasma States and Electrical Conductivity Showing Range of MHD Channel Conditions	9
Figure 2. Schematic of Explosively Driven Plasma Source	12
Figure 3. 120 MeV Flash Radiographs of Experiment 165-7	14
Figure 4. Faraday MHD Generator	15
Figure 5. Generator with Stainless Steel Resistive Load	18
Figure 6. Generator with External Graphite Resistive Load	19
Figure 7. High Power MHD Experiment	20
Figure 8. Schematic of the High Power MHD Experiment	21
Figure 9. Plasma Diagnostic Station	23
Figure 10. Flow Velocity and Electrical Conductivity for the 1-inch Diameter MHD Channel	29
Figure 11. MHD Generator Electrical Characteristics	32
Figure 12. Current, Load Voltage and Load Power (Experiment 165-7)	33
Figure 13. Current, Load Voltage and Load Power (Experiment 165-6)	36
Figure 14. Peak MHD Power Versus Applied B-Field	38
Figure 15. Peak MHD Power Versus Electrode Area	39
Figure 16. Trajectory of the MHD Channel Shock Showing its Interaction with the Generator	42
Figure 17. Post-Shot Electromagnet Coil Housing	43

Acknowledgement

The authors would like to acknowledge the valuable contributions throughout the program of our co-workers Mr. Thomas Bratton, Mr. Peter Krogh, Mrs. Beth Miranda, Miss Rita Rupp and Mr. Peter Vance. We also thank Mr. Kerry Bahl and the Bunker 851 test site crew at Lawrence Livermore National Laboratory (LLNL) for their enthusiasm and skill in fielding the MHD experiments.

The work presented in this report was sponsored by the Office of Naval Research Contract N00014-81-C-0045 under the direction of Dr. Bobby Junker and we gratefully acknowledge his encouragement and support. We are also indebted to Dr. Ed Florance and Mr. John Satkowski both formerly of ONR for their strong support of this research since its inception in 1975.

1.0 Introduction

This annual report summarizes the high power MHD experiments performed during the period 1 January 1981 to 30 June 1982. This work was the culmination of previous basic research programs dating back to 1975 on the characteristics of dense non-ideal plasmas and high magnetic Reynolds number MHD phenomena (References 1 to 5).

The primary objectives of this present effort were twofold. The first was to generate peak electrical power in the gigawatt range using an existing pulsed plasma source device. The second was to explore the scaling relationships of peak power with applied B-field and electrode area particularly as the electrical energy extracted becomes a significant fraction of the available plasma flow energy.

These objectives have been successfully met. Multi-gigawatt power levels have been achieved and the fundamental principles of this method of MHD power generation have been verified.

This work is leading to the development of an extremely compact, lightweight prime power source that can

deliver repetitively pulsed electrical power at gigawatt power levels and megajoule pulse energies. Pulsed plasma MHD technology is being considered for a number of important applications including prime power for laser, particle beam and microwave weapons, electromagnetic launchers and high power emergency communications.

2.0 Pulsed Plasma MHD

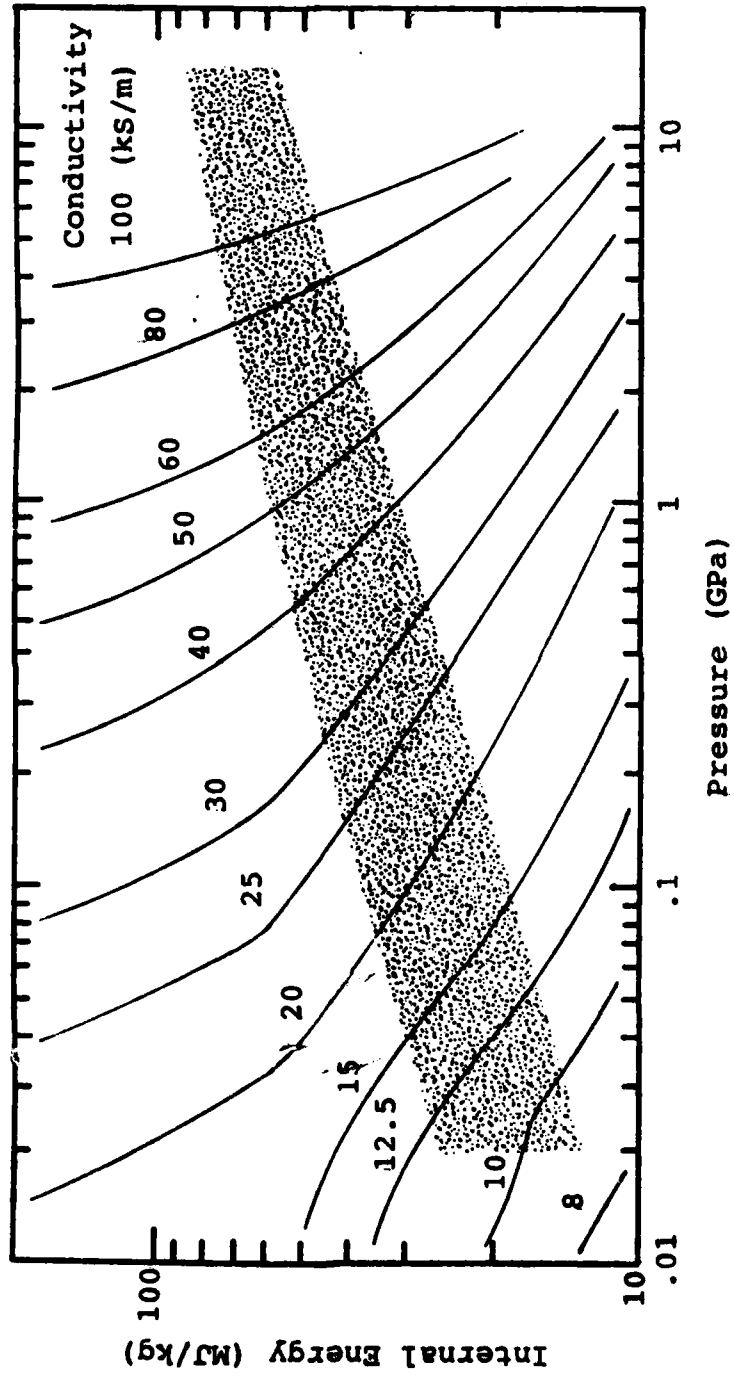
2.1 Plasma States

Pulsed plasma MHD is distinguished from other MHD power generation methods by the plasma states achieved in the generator. The dense non-ideal plasma flow is characterized by considerably higher flow velocities (10 to 30 km/s) and electrical conductivities (15 to 30 kS/m) than the more familiar high power combustion MHD generators. A further distinguishing feature is the high magnetic Reynolds number* at which the pulsed plasma MHD generator is operated. In the present program, experiments have been conducted at magnetic Reynolds numbers of up to 35. The predicted field perturbation effects were measurable but by design did not degrade generator performance. Both the question of dense non-ideal plasma conductivity and high magnetic Reynolds number generator operation have been thoroughly addressed in previous work (References 2 and 4).

The argon plasma states encountered in our MHD work are shown in Figure 1. The electrical conductivities

*Magnetic Reynolds Number
based on MHD channel
diameter $R_m = \sigma \mu_0 u d$

where σ = electrical conductivity
 μ_0 = permeability of space
 u = flow velocity
 d = channel diameter



1980

Figure 1 Argon Plasma States and Electrical Conductivity Showing Range of MHD Channel Conditions

are calculated using the Rogov formulation (Reference 6) and a modified Debye-Huckel equation-of-state appropriate for the dense non-ideal conditions in the MHD channel (Reference 7). These conductivities are in substantial agreement with more detailed calculations being carried out at the Lawrence Livermore National Laboratory (LLNL) (Reference 8). They are also supported by our own measurements of plasma conductivity which are presented in the subsequent discussion of results.

The conditions in the plasma source are characterized by pressures up to 20 GPa and near metallic densities. In this regime we have used a comprehensive equation-of-state provided by LLNL (Reference 9). This agrees well with the modified Debye-Huckel equation-of-state at the lower density conditions encountered in the MHD generator.

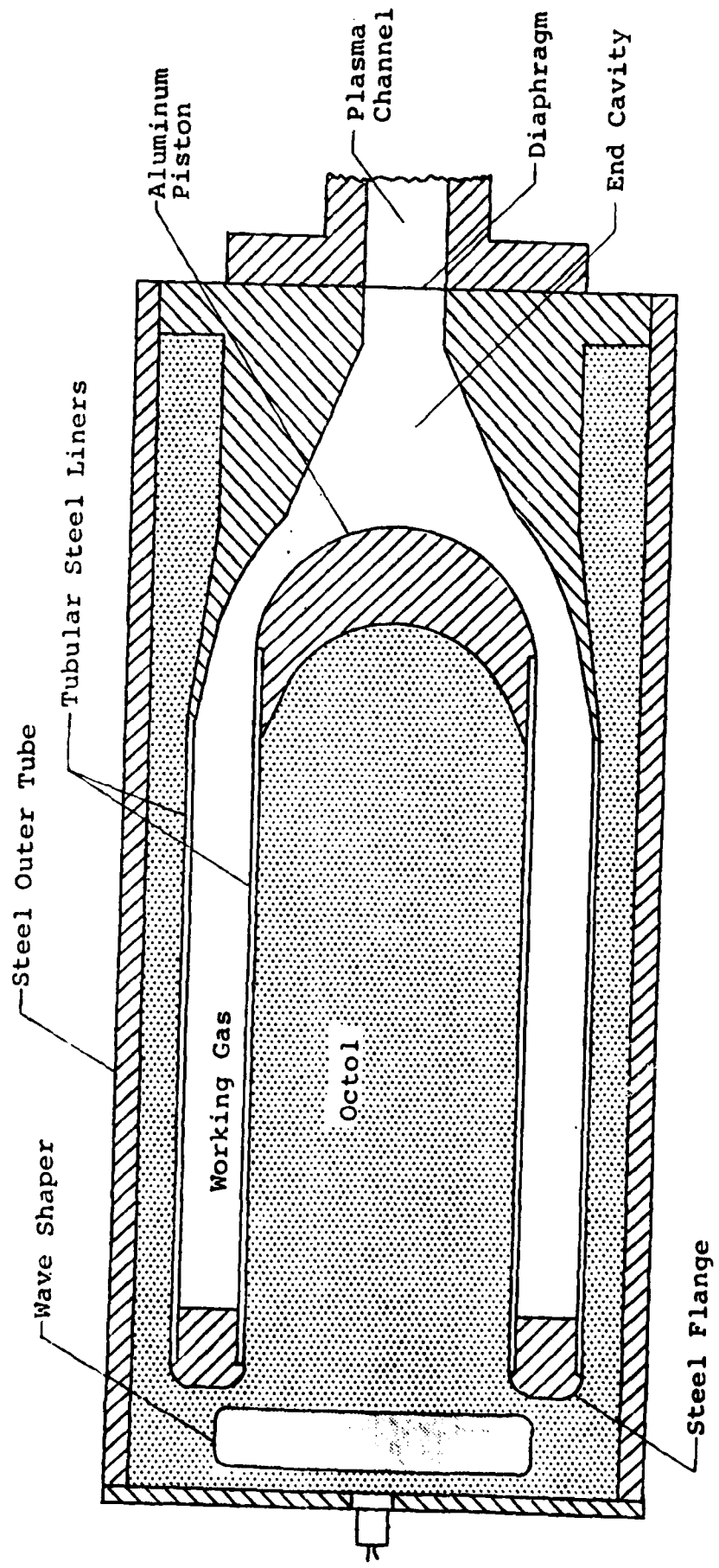
We have devoted considerable effort to calculating the plasma energization in the plasma source and its subsequent expansion down the MHD channel. These calculations use the LLNL equation-of-state and are closely matched to the observed performance of the plasma source and to the measured velocities and conductivities in the MHD channel. The range of calculated MHD channel conditions typical of our experiments are also shown in Figure 1.

Argon was used as the working fluid in the present high power MHD experiments. In the past we have also used xenon and air with measured conditions comparable to those encountered in the argon experiments (References 3 and 5).

2.2 Plasma Source

In our MHD device, the first energy conversion process is from chemical energy of the explosive to plasma energy. The energy of the explosive (5.3 MJ/kg) is concentrated to produce an energetic plasma (100 MJ/kg) which can thereupon expand to high velocities (20 km/s) while maintaining the required electrical conductivity (30 kS/m) for efficient generator operation.

The plasma source is shown in cross-section in Figure 2. Octol explosive is cast around a steel lined annular region containing the pressurized working gas. By means of a wave shaper the detonation front is caused to pass simultaneously along the outer and inner liners progressively collapsing the annular volume. The impact of the liners forms a dynamic seal which moves at the explosive detonation velocity and drives a strong, high pressure shock into the working gas. The result is a transfer of approximately 25% of the explosive energy into the shocked plasma.



1420A

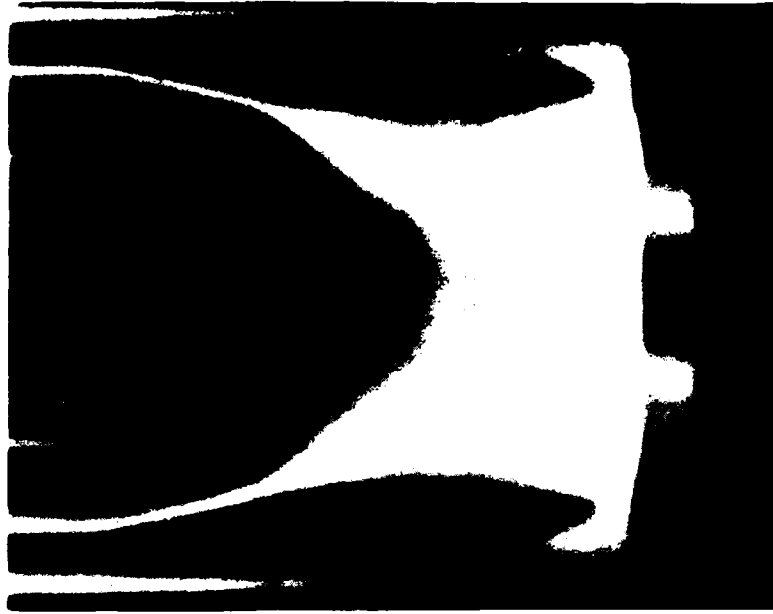
Figure 2 Schematic of Explosively Driven Plasma Source

The plasma now moving at the detonation velocity of the explosive converges into the end cavity and is further energized by an aluminum piston driven by the inner cylinder of explosive. The piston continues collapsing the cavity volume driving the plasma into the MHD channel.

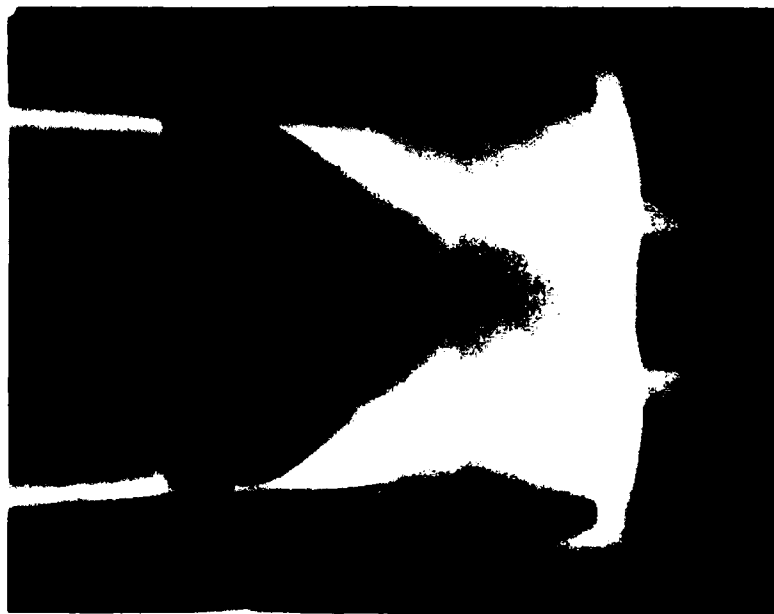
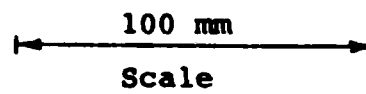
The operation of the plasma source is illustrated by the 120 MeV flash X-rays presented in Figure 3. The upper photograph shows the end cavity and MHD channel inlet region prior to initiation of the explosive. The lower photograph is taken just after completion of the collapse of the steel liners. All the plasma has been driven into the end cavity. The aluminum piston has been in motion for 3.8 μ sec. After another 15 μ sec the injection of plasma into the MHD channel will have been completed.

2.3 Faraday Mode MHD Generator

The plasma generated by the source flows down the channel and passes between a pair of electrodes typically 15 to 40 diameters downstream of the channel inlet. In the present experiments an externally energized electromagnet field coil surrounds the electrode region and provides a reasonably constant transverse magnetic field in the volume between the electrodes (Figure 4a). The

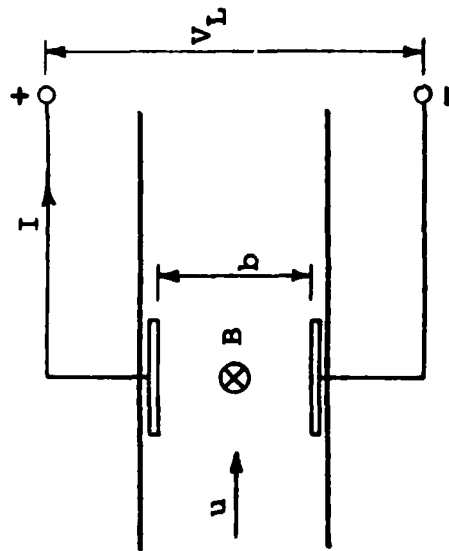


a) Set-up



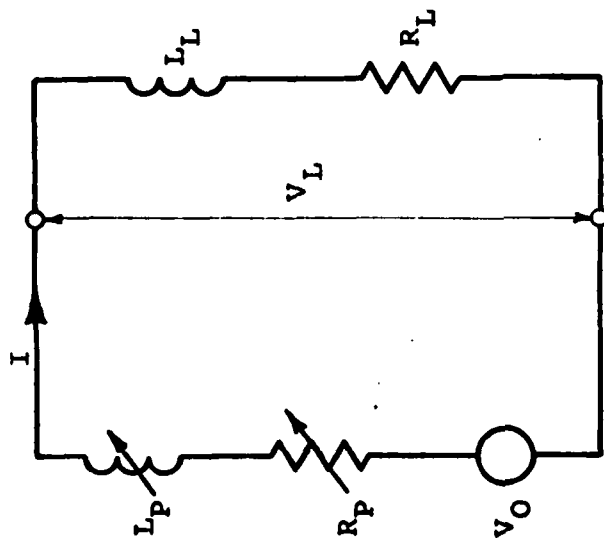
b) 3.8 μ sec after first motion
of aluminum piston

Figure 3 120 MeV Flash Radiographs of Experiment 165-7 1447



a) Simplified Schematic of Faraday MHD Generator

- B = Magnetic Field
- u = Plasma Flow Velocity
- b = Electrode Separation
- σ = Plasma Conductivity
- A = Electrode Area
- L_p, L_L = Plasma, Load Inductance
- R_p, R_L = Plasma, Load Resistance
- V_O = Open Circuit Faraday Voltage
- I = Current



b) Faraday Generator Circuit Model

$$V_L = R_L I + L_L \frac{dI}{dt}$$

$$V_O = B u b$$

$$R_p = \frac{b}{\sigma A}$$

$$V_O = V_L + R_p I + R_L \frac{dI}{dt}$$

MHD generator can be accurately represented by a simple lumped parameter circuit model (Figure 4b). The measured load voltages and current are consistent with the circuit model and the measured values of its elements.

In practice, circuit inductances can be kept very small (1 or 2 nanohenries). Plasma resistance is on the order of a few tenths of a milliohm making this a very low impedance generator. Near peak power conditions, the inductive voltage drops are negligible and the circuit equation of Figure 4b can be rearranged to express the power in a matched load ($R_L=R_p$) as:

$$\begin{aligned} P &= I^2 R_L = \frac{B^2 u^2 b \sigma A}{4} \\ &= \frac{B^2 u A}{4 \mu_0} R_m \end{aligned} \quad (1)$$

where R_m = magnetic Reynolds number

This derivation neglects any perturbation in the applied B-field at high magnetic Reynolds numbers. Magnetic Reynolds number effects on generator open circuit voltages have been theoretically estimated in Reference 4 and routinely measured in laboratory calibration experiment (References 2, 3 and 5). For magnetic Reynolds numbers less than 50 as in the case in the present experiments, the generator design can be readily modified to operate in accordance with the simple circuit model of Figure 4a.

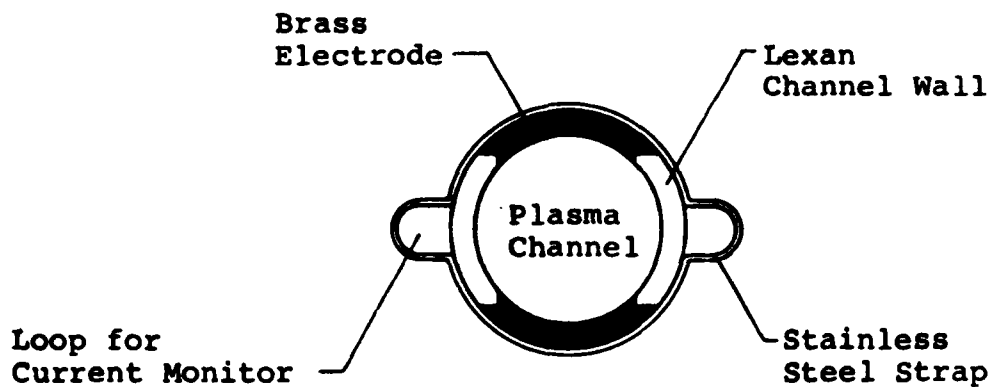
In the MHD experiments reported herein the electrodes were attached directly to a matched resistive load. In the lower power density experiments the load was formed by a stainless steel strap mounted just outside the MHD channel. Such a load is shown in Figure 5.

In the higher power density experiments, the current was conducted by a low inductance strip-line through the field coil to an externally mounted carbon resistive load with enough mass to absorb the Joule heating without large changes in load resistivity. An externally mounted load configuration is shown in Figure 6.

2.4 Experimental Arrangement and Diagnostics

A typical MHD experiment is shown in Figure 7 with the essential elements illustrated schematically in Figure 8. A 200 kJ capacitor bank installed at the LLNL explosive test site is used to drive the field coil for the MHD generator. An identical bank in the Artec laboratory is used to test and calibrate the field coils.

The plasma source diagnostics consist of a 120 MeV flash radiograph to view the internal operation of the plasma source; ionization pins to monitor the explosive detonation velocity; and a photodiode to determine diaphragm rupture time.



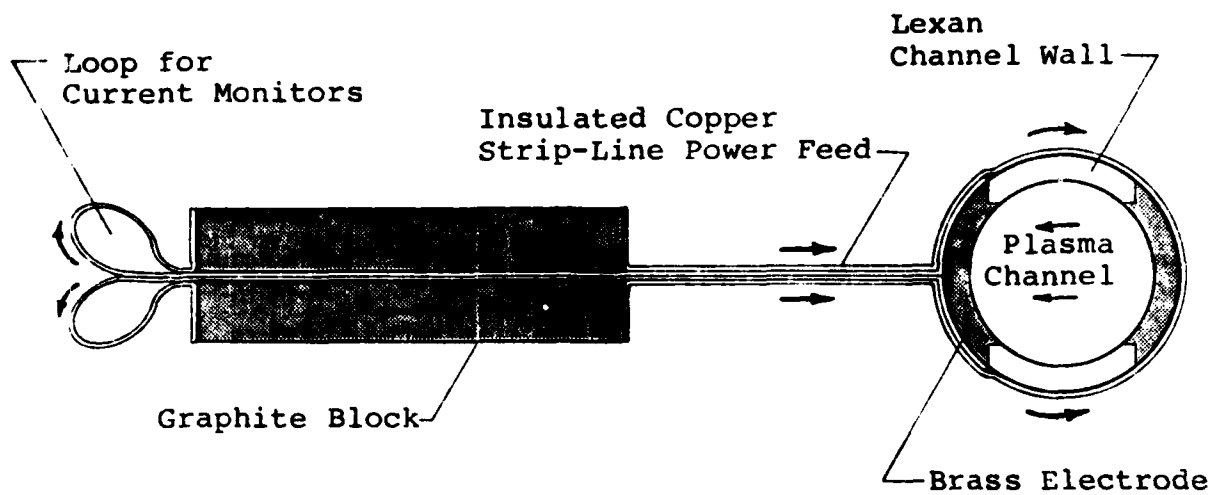
a) End View of Generator Showing Stainless Steel Strap Used as a Resistive Load



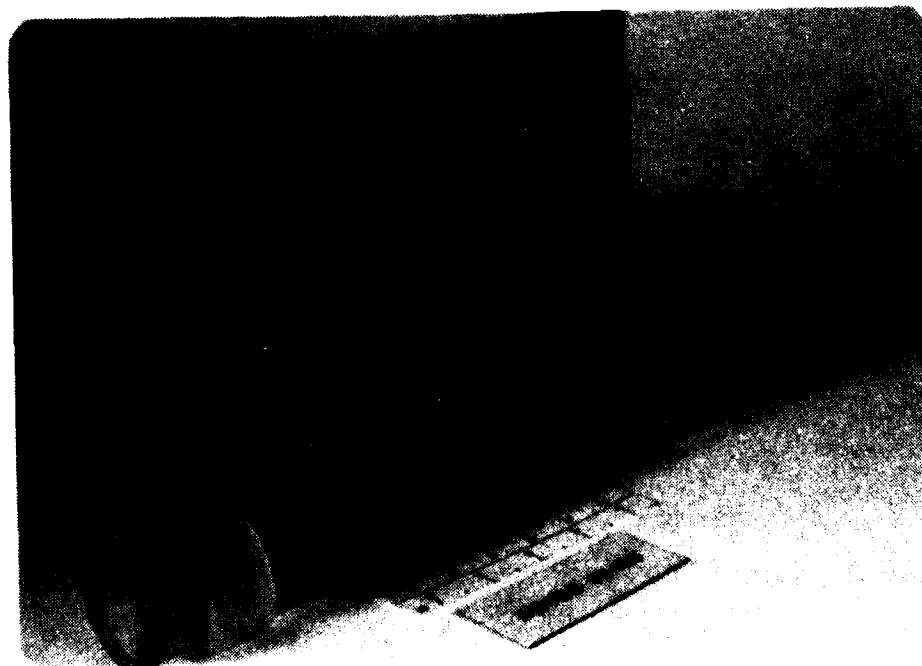
b) Generator Section with Diagnostics Attached

Figure 5 Generator with Stainless Steel Resistive Load

1439



a) End View of Generator with External Graphite Resistive Load



b) Generator Section

Figure 6 Generator with External Graphite Resistive Load

1440

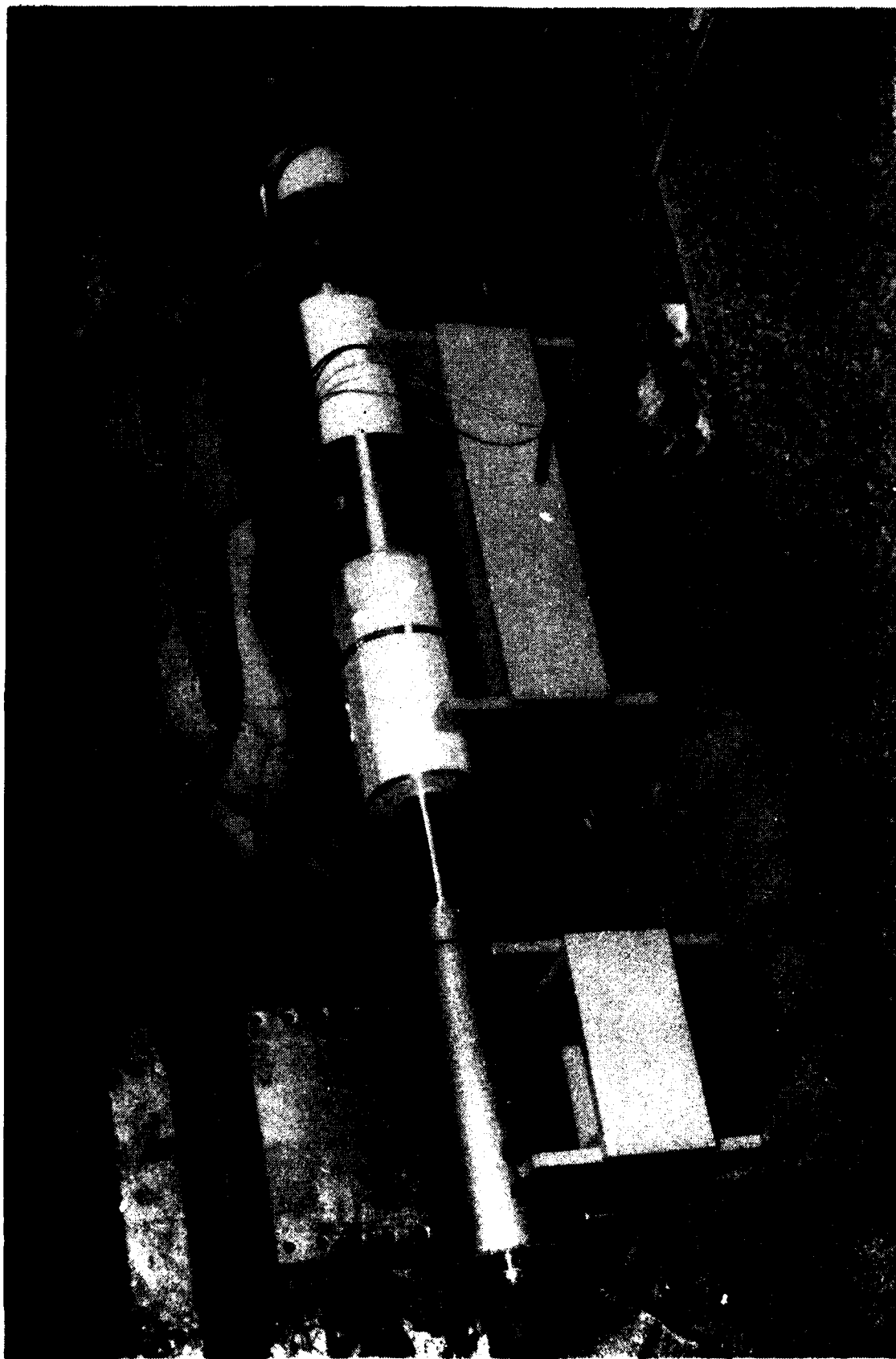
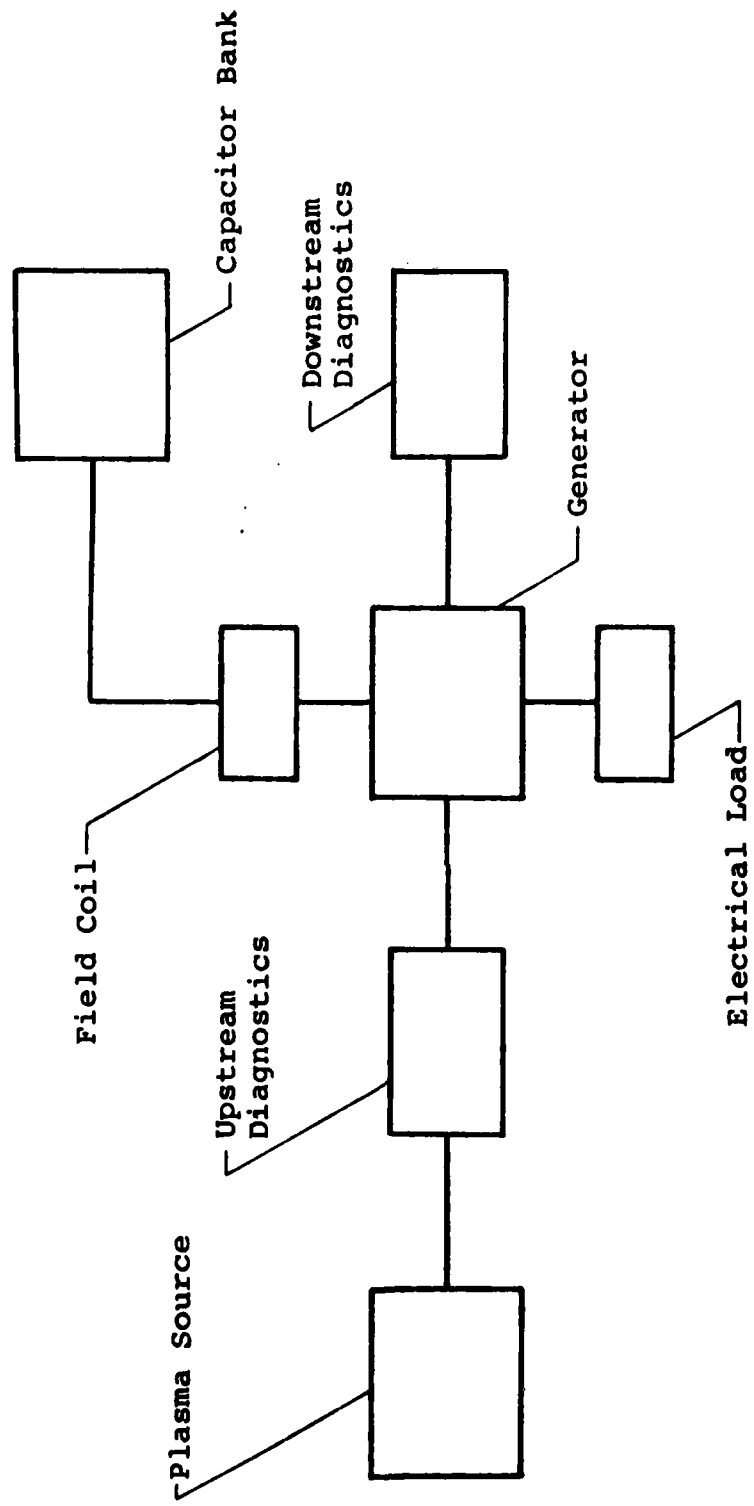


Figure 7 High Power MHD Experiment

1441



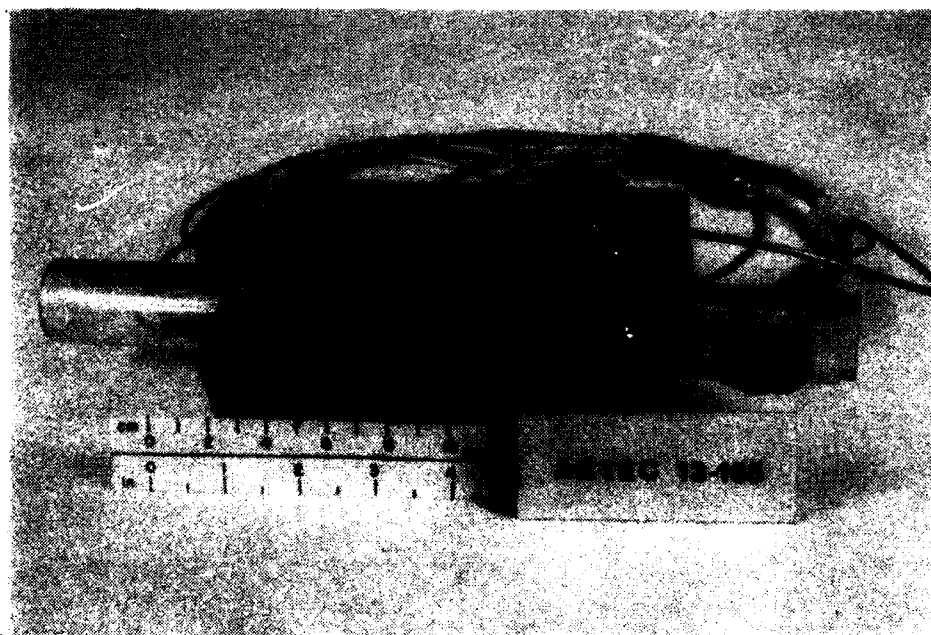
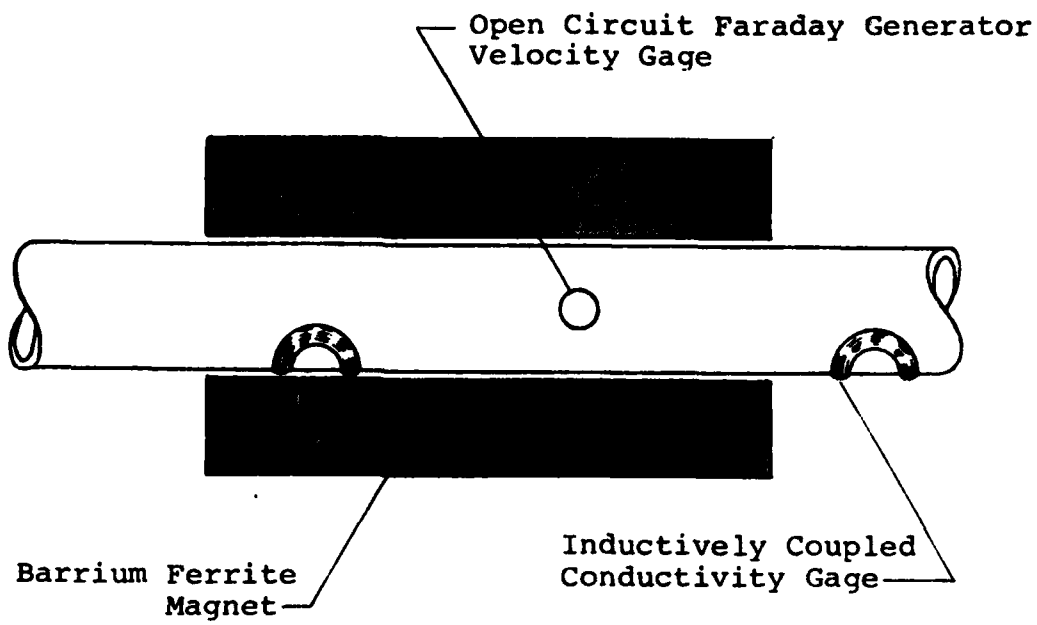
M52

Figure 8 Schematic of the High Power MHD Experiments

Three types of diagnostics are used to measure the plasma properties in the channel. Plasma flow velocity histories are monitored by means of an open circuit Faraday generator using small permanent magnets to provide the field. Plasma conductivity histories are measured inductively with search coils placed near the ends of the permanent magnets. These search coils are calibrated in the laboratory to obtain coil output as a function of magnetic Reynolds number. A typical diagnostic station for velocity and pickup coil conductivity gages is shown in Figure 9. Plasma resistivity is also determined from the circuit equation of Figure 4b using the measured circuit current, load resistance, circuit inductances and open circuit voltage within the generator. A detailed description of the theory and operation of these diagnostics is available in References 3 and 5.

Attempts were made to measure pressure histories in the MHD channel. These proved to be difficult in the pulsed field environment of the MHD generator and electromagnet field coil, and the measurements were ambiguous.

The power generated in the load is determined directly from the measured voltages and current in the load. Voltage measurements are made in several locations across the load to detect any variations in current density.



1448

Figure 9 Plasma Diagnostic Station

Current is measured by a calibrated integrating pickup coil placed in a loop in the current path. Load resistance, inductance and plasma channel inductance are measured in the lab before the experiment. In the analysis of the experiments account is taken of changing load resistance due to Joule heating and of the variable plasma resistance and inductance as the plasma sweeps across the electrodes.

All the plasma channel and load diagnostics together provide a detailed time-distance record of the leading edge of the plasma pulse.

The output of the B-field coil is monitored by a capacitor bank current measurement and by a calibrated pickup loop in the field coil housing. The B-field generated inside the electrode volume is independently determined by a small open circuit Faraday generator placed just upstream of the electrodes in the main magnetic field.

3.0 High Power MHD Experimental Results

In addition to numerous design and calibration tests carried out in the Artec laboratory, seven experiments were conducted at explosive test sites. The purpose and general results of each of the seven tests are given in Table 1.

A common plasma source design was used in tests 165-2 through 165-6 to drive a 25.4 mm diameter channel. A 38.1 mm diameter channel and modified plasma source was used in the final experiment 165-7. Experiments 165-3 through 165-7 were full MHD power tests. The highest peak power (6 GW) and delivered energy (140 kJ after 35 μ sec) of the program were measured in the final experiment. Table 2 summarizes the B-field, electrode area, power and energy associated with each test.

3.1 Plasma Flow Conditions

Both velocity and search coil conductivity history measurements were made in a small B-field provided by permanent magnets as described in Section 2.4. Great care was taken to isolate these diagnostics from the fields generated by the electromagnet and the MHD currents.

Experiment	Purpose	Results
165-1	Technology experiment for data on plasma source components	Key data for plasma source design and modelling calculations
165-2	Experiment to measure plasma source output and MHD channel flow conditions	120 MEV x-ray and ion pin data confirms expected plasma source performance
165-3	First full MHD experiment. 2T applied field, several small electrodes	Achieved expected results, first hint of generator-flow interaction
165-4	Increase applied B-field to 4T and increase electrode length	Field coil internal short results in higher than expected B-field. Flow interaction is apparent
165-5	5.5T applied field and increased electrode length	Achieved expected results. Stainless steel load melts at 20 μ sec
165-6	First test of external carbon resistive load	Achieved expected results with heavily diagnosed load. Strip-line evens out current distribution
165-7	External load, increased channel diameter to get more flow energy	Flow velocity and conductivity reduced slightly. Highest load power and energy achieved

Table 1. Description of Major Experiments

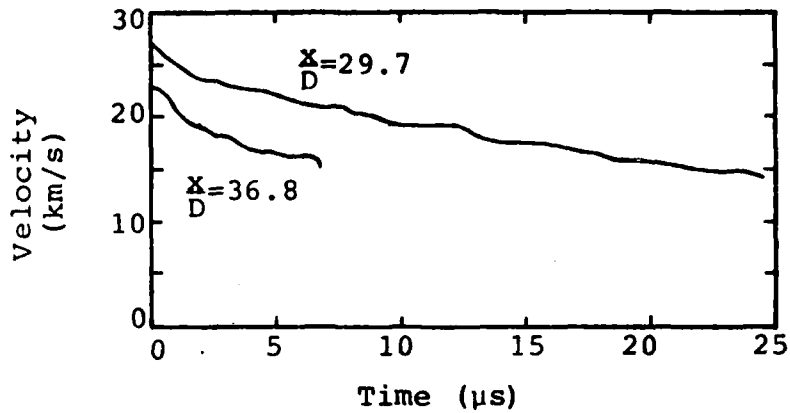
Experiment	Channel Diameter (mm)	B-field (teslas)	Electrode Area (mm ²)	Nominal Load Resistance (milliohms)	Peak Load Power (gigawatts)	Energy* to Load (kilojoules)	Average* Load Power (gigawatts)
165-3	25.4	2.1	400	1.55	.080	1.5	.060
		2.1	400	1.70	.140	2.0	.078
		2.1	400	1.59	.130	1.9	.075
		2.1	<u>800</u>	.832	<u>.210</u>	<u>3.6</u>	<u>.144</u>
Total			2000		.560	9.0	.357
165-4	25.4	5.2	400	.827	.720	9.0	.360
		5.2	<u>1600</u>	.263	<u>2.700</u>	<u>28.0</u>	<u>1.100</u>
Total			2000		3.420	37.0	1.460
165-5	25.4	.080	400	2.41	1.6×10^{-4}	.0025	1×10^{-4}
		5.22	2400	.209	3.75	47	1.85
165-6	25.4	4.3	2400	.473	2.70	41	1.65
165-7	38.1	5.6	4800	.357	6.07	105	4.20
						140**	4.0

*based on 25 μ sec pulse
**based on 35 μ sec pulse

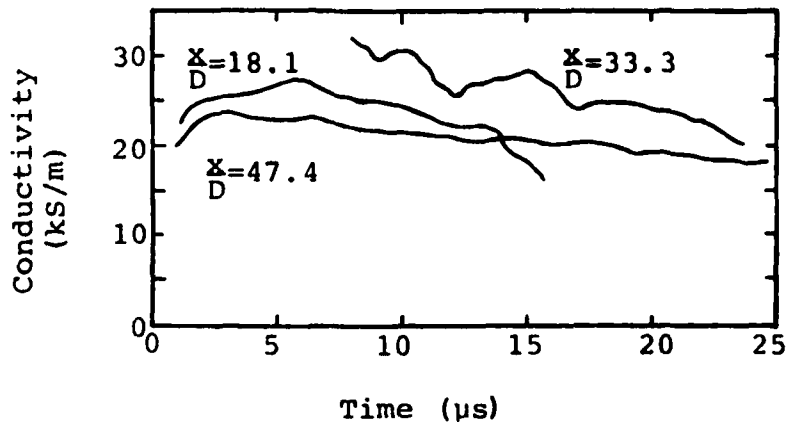
Table 2. Summary of Results for Full MHD Experiments

Flow velocity histories upstream ($\frac{x}{D}=29.7$) and downstream ($\frac{x}{D}=36.8$) of the MHD generator ($30.9 < \frac{x}{D} < 35.7$) are shown in Figure 10. The upstream velocity history with a peak flow velocity of 27 km/sec is representative of experiments 165-2 through 165-6. The downstream velocity history is influenced by the MHD generator both through Lorentz force braking and Joule heating and is thus different for each experiment. With higher levels of MHD power generation, the downstream velocities are reduced as flow kinetic energy is converted to electrical energy in the load and internal energy in the plasma.

The upstream conductivity history ($\frac{x}{D}=18.1$) shown in Figure 10 is representative of experiments 165-2 through 165-6. The downstream history ($\frac{x}{D}=47.4$) is influenced by power extraction in the generator. With little or no power generation, conductivity falls with distance down the channel as the flow expands (see Reference 5 for examples). In the present high power experiments where the energy extracted is a significant fraction of the available flow energy, Joule heating adds measurably to the plasma internal energy. The result is that conductivity either decreases less rapidly with distance or, in the highest power experiments, exhibits an increase just downstream of the generator.



a) Velocity Histories Experiment 165-6 (electrodes extend from $\frac{x}{D}=30.9$ to $\frac{x}{D}=35.7$)



b) Conductivity Histories Experiment 165-6¹⁹⁸⁴
(search coil conductivities at $\frac{x}{D}=18.1$ and 47.4)

Figure 10 Flow Velocity and Electrical Conductivity for the 1-inch Diameter MHD Channel

In the final experiment 165-7 the channel diameter was increased to 38.1 mm. The resultant peak velocity and peak conductivity were reduced by about 10%. However the time rate of decrease of both velocity and conductivity was less than observed in previous experiments.

In past work (References 3 and 5) loaded Faraday generators operating in a small B-field provided by permanent magnets were used to directly measure plasma resistance and hence plasma conductivity. In general the plasma conductivity measured in this way was a third to one half the conductivity measured inductively by the search coils. The difference was ascribed to a resistive interface between the plasma and the electrode surface which affects the direct resistance measurement more than the inductive measurement.

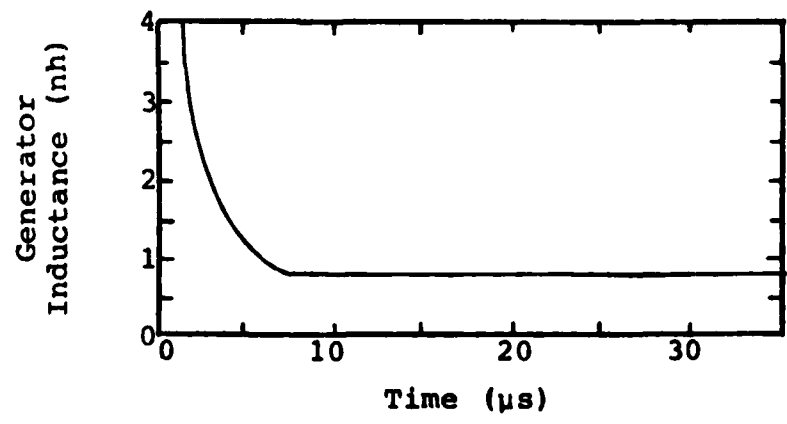
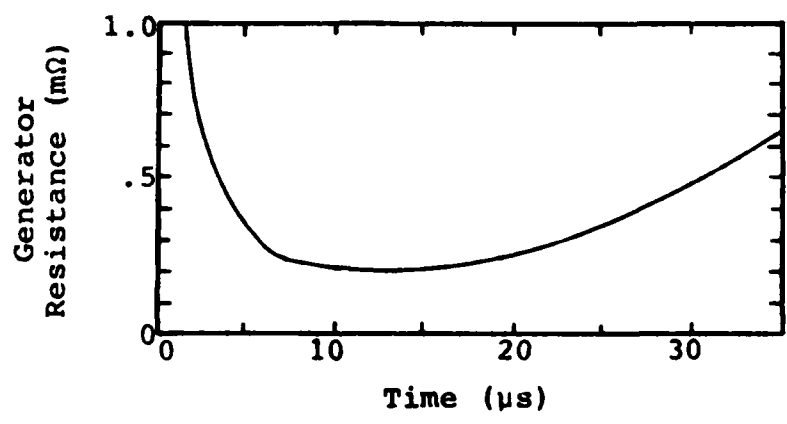
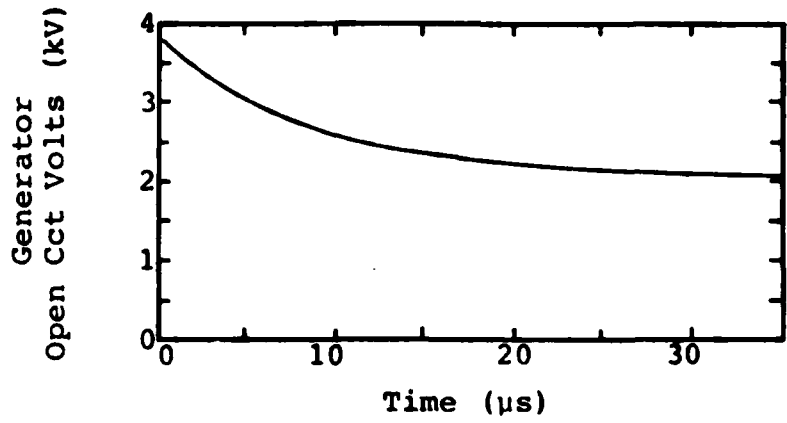
In the present high power experiments, the direct ($\frac{x}{D}=33.3$) and inductive conductivity determinations were, within the error of measurement, almost identical. It is surmised that the large current densities (up to 8×10^8 A/m²) breakdown the interface resistance so that the direct and inductive measurements of conductivity are now representative of the core flow.

3.2 MHD Generator Performance

In pulsed plasma MHD, generator voltage is a maximum as the flow sweeps across the electrodes and it decreases thereafter. Generator inductance achieves a minimum when the flow reaches the downstream edge of the electrode and is constant thereafter. Generator resistance reaches a minimum when the product of plasma density and internal energy is maximized several diameters behind the shock front. MHD generator voltage, resistance and inductance characteristics derived from the results of experiment 165-7 are shown in Figure 11.

Load inductance is constant but load resistance increases with Joule heating. In the case of the carbon resistive loads used in the latter experiments load resistance varies both with Joule heating and with magnetoresistive effects at high current densities. In general the load resistances were designed to be approximately matched to generator resistance at the time of peak power.

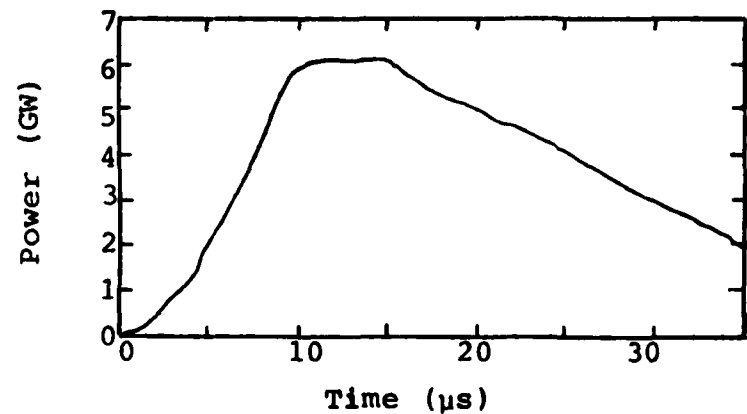
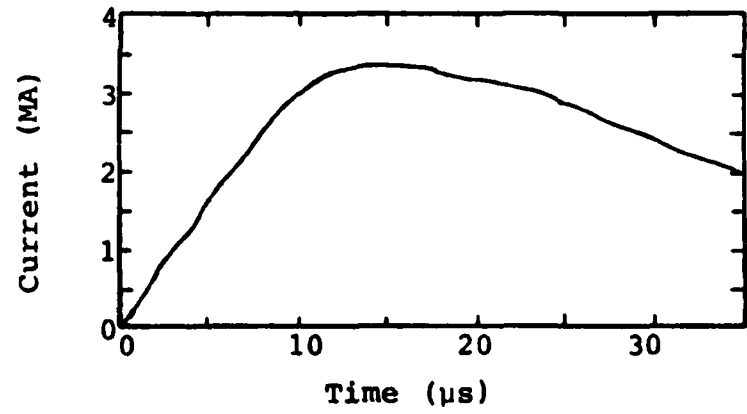
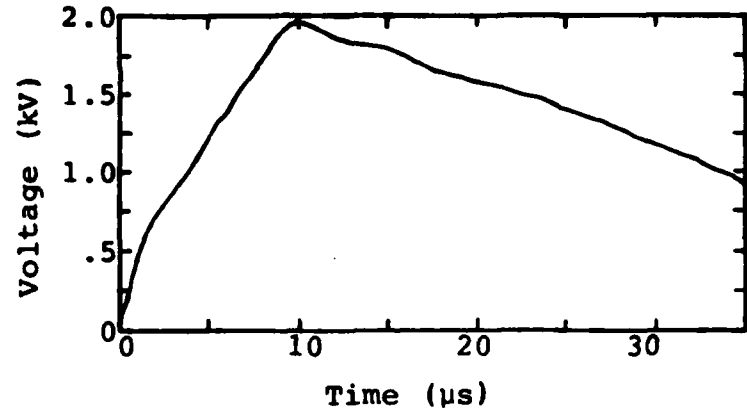
Typical current and load voltage traces and the corresponding load power (measured volts times measured current) are shown in Figure 12. These illustrate the waveforms characteristic of pulsed plasma MHD in a constant applied B-field. They also illustrate the high current, low impedance nature of the generator.



1433

6 tesla B-field, 38.1 mm diameter channel,
160 mm long electrodes

Figure 11 MHD Generator Electrical Characteristics



1437

Figure 12 Current, Load Voltage and Load Power (Experiment 165-7)

As shown in Table 2, several small closely spaced but electrically separate electrodes were tested in experiment 165-3 to observe any interactive effects between electrodes when connected by the conductive plasma. Within the resolution of our diagnostics we saw none. The peak power achieved in the upstream load was low (see Table 2) because the applied B-field was diminished by magnetic Reynolds number effects, this electrode being positioned close to the upstream edge of the applied field.

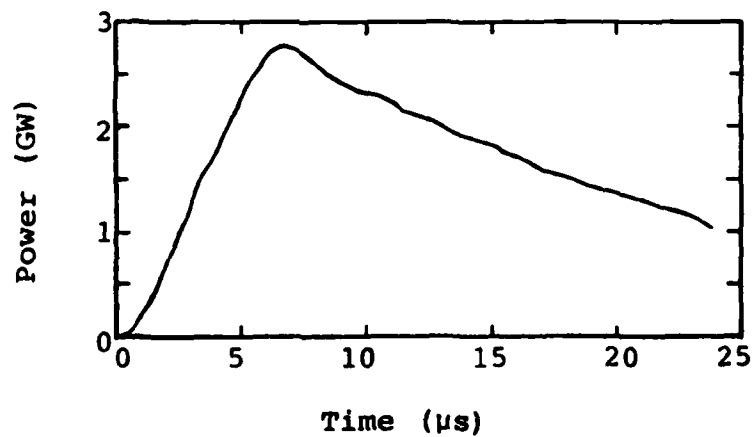
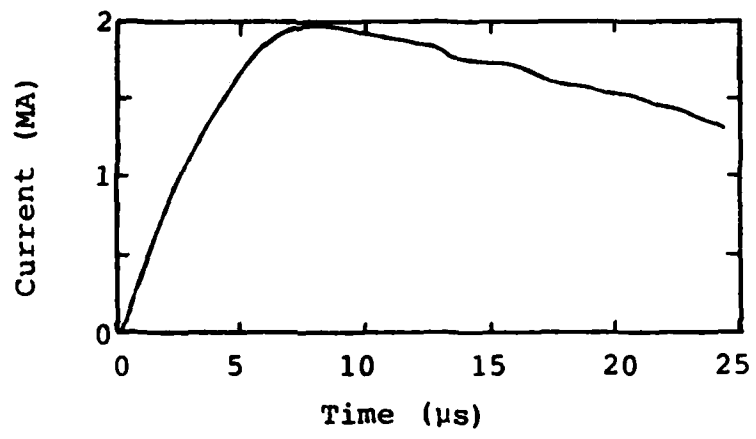
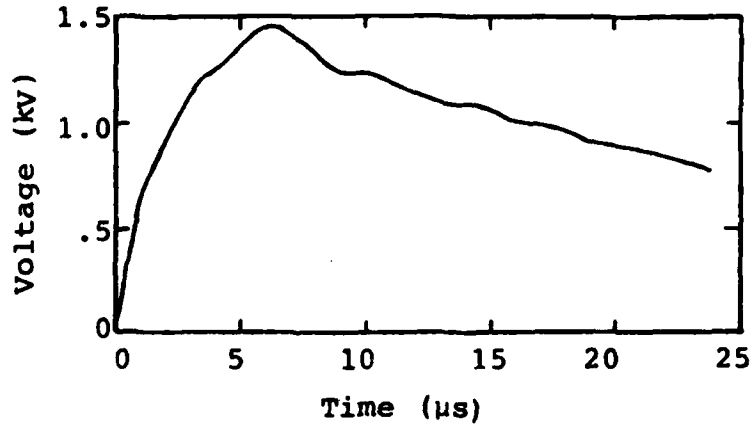
In experiments 165-4 and 165-5 parallel stainless steel loads such as shown in Figure 5 were used. It was calculated that these loads would melt after 20 μ sec although the event was not noticeable from load voltage and current records. Voltage monitors at upstream, middle and downstream positions on the load revealed current distributions along the load especially as the plasma pulse first sweeps across the electrodes. The current tends to flow circumferentially around the load rather than spreading out longitudinally which is a much higher inductance current path. Thus there is very little perturbation of the applied B-field by the nearly orthogonal fields created by the load currents.

Experiment 165-6 was the first test of a carbon resistive load mounted outside the electromagnet. The load

was sufficiently massive to minimize resistance change from Joule heating. Current was conducted from the electrodes to the load by a low inductance strip-line. The short strip-line permitted the current to distribute itself evenly across the load as was confirmed by upstream, middle and downstream load voltage measurements. The measured current, load voltage, and load power are shown in Figure 13. The B-field in the generator was lower than the design goal of 5.5 tesla because of shielding by the one piece copper strip-line and electrodes.

In experiment 165-7 the lower electrode and strip-line were segmented to allow rapid penetration by the externally applied B-field (see Figure 6). In this experiment the large load current densities (up to 8×10^8 A/m²) gave rise to a substantial magnetoresistive effect in the load. At peak power, the load resistance was about 3 times higher than the plasma resistance. The measured load power of 6 GW was thus less than the anticipated 8 GW for matched conditions.

Because of the larger channel diameter in this final experiment, the pulse widths were longer and the measured energy delivered to the load in 35 μ sec was 140 kJ. The current, load voltage and load power for this experiment are shown in Figure 12.



1496

Figure 13 Current, Load Voltage and Load Power (Experiment 165-6)

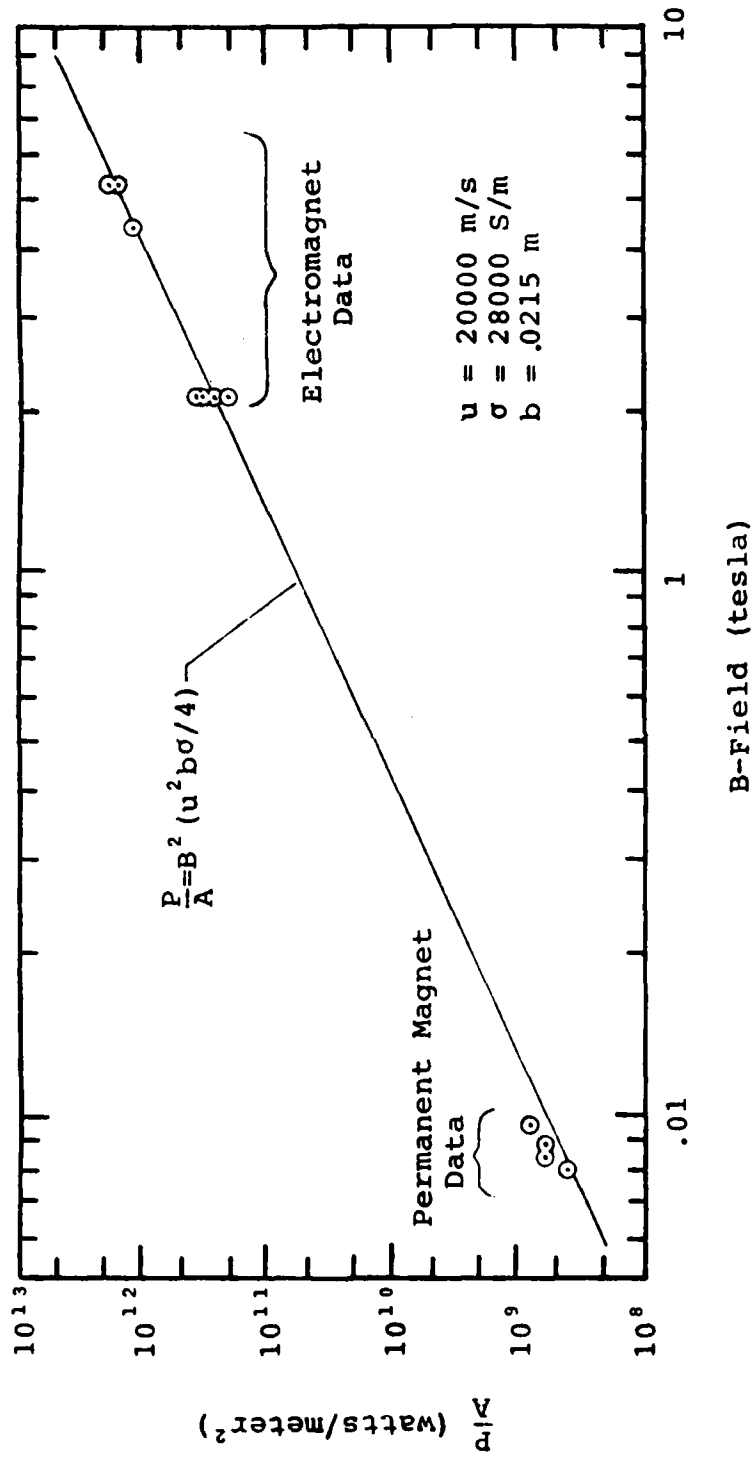
3.3 Scaling Relationships

According to equation (1) peak power should scale directly with electrode area and as the square of the applied B-field. These scaling relationships are confirmed by the data from the present experiments and the low B-field data of Reference 5. These data cover a B-field range of .08 tesla to 5.22 tesla and an electrode area range of 97 mm² to 2400 mm² (Figures 14 and 15). These data were taken from experiments using the same plasma source design and the same 25.4 mm diameter MHD channel design.

At peak load power, the inductive voltage drops in the circuit are negligible and equation (1) can be plotted using measured values of velocity and conductivity at the time of peak power. Equation (1) is shown in both Figures 14 and 15 demonstrating that not only does the data scale as predicted but that the magnitude of peak power can be accurately predicted by the circuit model of equation (1).

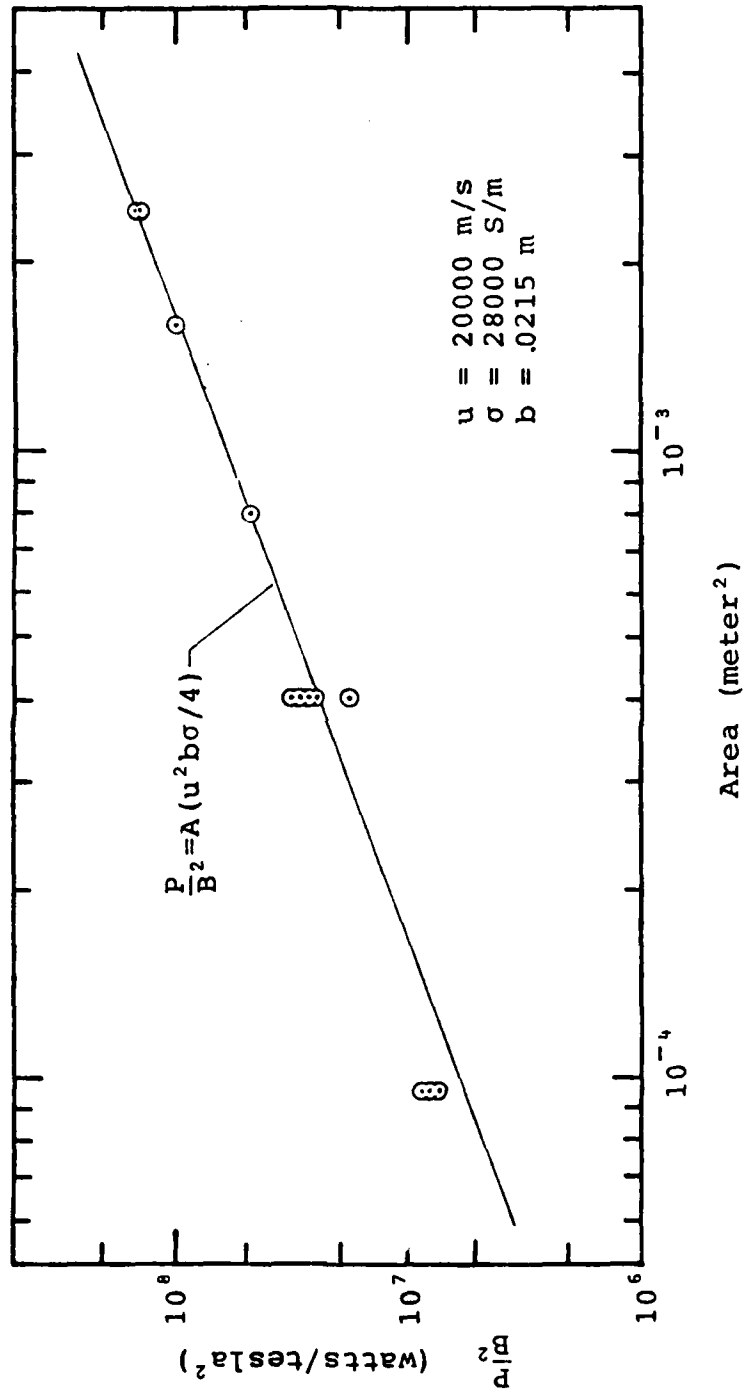
It should be noted that equation (1) does not include the following second order effects when used to plot the data.

- fringing of the electric fields tends to increase the effective electrode area. The effect is



1449

Figure 14 Peak MHD Power Versus Applied B-Field



1448

Figure 15 Peak MHD Power Versus Electrode Area

greatest for the small electrode data

- when peak power is measured, there can be a substantial velocity gradient along the electrodes. The effect is greatest for the large electrode data (the largest electrodes are more than 6 channel diameters long)
- interaction between the electric circuit and plasma flow tends to reduce flow velocity and increase plasma conductivity. In the present experiments the effect is greatest for the highest applied B-field data
- equation (1) was plotted assuming equal load and plasma resistances. At peak power in several experiments, load resistance was often more than two times plasma resistance

3.4 Electric Circuit-Plasma Flow Interactions

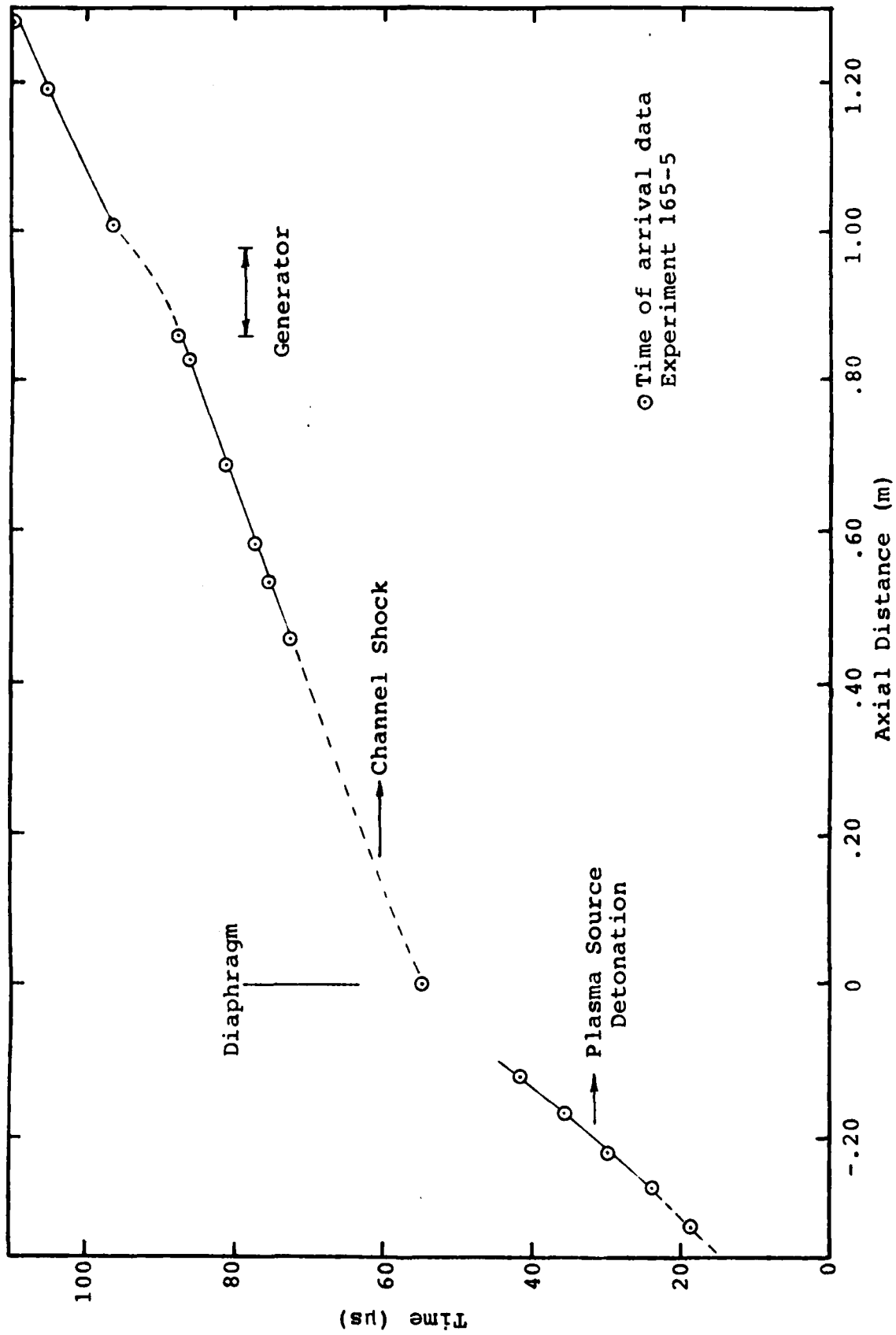
Most of the energy of the plasma in the MHD channel is in the form of kinetic energy. As the plasma flows through the applied magnetic field it is decelerated by the magnetic (Lorentz) forces. This converts kinetic energy of the flow to electrical energy in the load and

to internal energy of the plasma which is a resistive element in the electrical circuit. When the electrical energy extracted is a significant fraction of the incoming flow energy, the plasma is heated and slowed resulting in a rapid rise in pressure and formation of an upstream running shock.

In the present experiments, moderate interactions were observed in all the experiments. These ranged from subtle manifestations in the low-field small-electrode experiment 165-3 to definite flow perturbations in the high-field large-electrode experiments 165-4 through 165-7.

In these latter experiments, the flow velocities downstream of the MHD generator were reduced (Figure 10). The time of arrival data for the leading edge of the plasma pulse unambiguously illustrate the magnetic braking of the flow by the generator as shown in Figure 16.

The increased conductivities measured downstream (Figure 10) also reflect an increase in internal energy of the plasma as a result of Joule heating. This was further evidenced by a recovered electromagnet housing which was overexpanded on the downstream end by increased internal pressure (Figure 17).



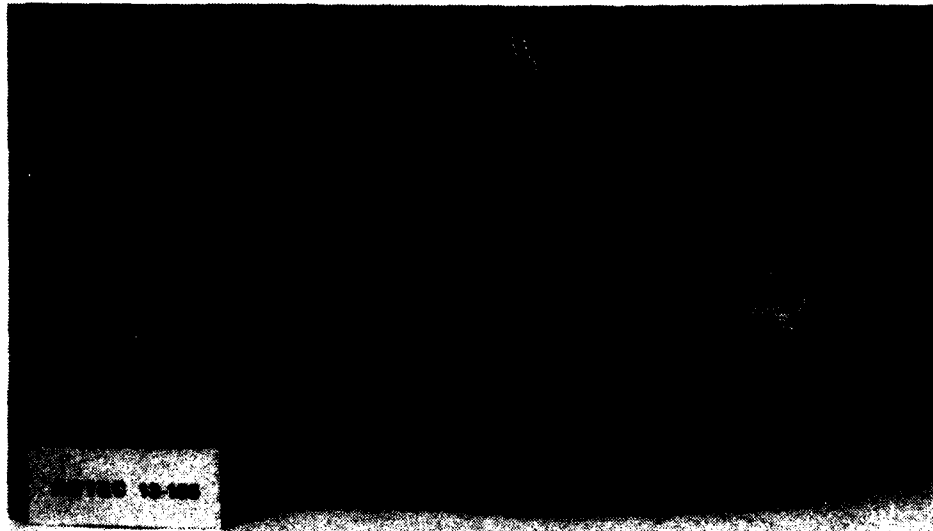
1419A

Figure 16 Trajectory of the MHD Channel Shock Showing Its Interaction with the Generator

Direction of Flow



100 mm
Scale



1442

Figure 17 Post-Shot Electromagnet Coil Housing

3.5 Effect of MHD Channel Diameter

The diameter of the MHD channel in the final experiment 165-7 was increased by 50% to 38.1 mm to utilize more of the plasma generated by the plasma source. Flow velocities and conductivities were reduced by approximately 10% because of the smaller convergence ratio from the plasma source to the MHD channel. The duration of the plasma pulse was increased and a larger mass of energetic plasma participated in the MHD process. With the 50% increase in electrode separation, there is a comparable increase in the generator driving voltage. As a result of this and the increased plasma energy, substantially more electrical energy was delivered to the load at higher power levels than in previous experiments using the same plasma source.

4.0 Conclusions

In past programs Artec Associates has carried out theoretical and experimental work to determine properties of dense non-ideal plasmas generated by an explosively driven plasma source. Concurrent theoretical and experimental programs demonstrated that MHD Faraday generators could be operated effectively at magnetic Reynolds numbers in excess of 50. These efforts led to the conclusion that gigawatt power levels could be achieved in a compact pulsed plasma MHD system with applied magnetic fields of several tesla.

In the present program peak electrical powers in excess of 2.5 GW were attained in four of the five full MHD experiments. A peak power of 6 GW with a delivered pulse energy of 140 kJ was achieved in the final experiment with an applied field of 5.6 tesla.

A major scientific objective of this program was to verify the scaling relationships of peak power with applied B-field and electrode area. As anticipated, peak power varies as the square of the applied B-field and directly as the electrode area over a wide range of conditions. These relations are valid when the electrical energy generated is a small fraction of the plasma flow energy. In

the present experiments deviations from these scaling relations were measurable when the energy extracted was estimated to be 10 to 20% of the available flow energy.

The scaling relations are derived from an analysis based on a simple lumped parameter circuit model for the MHD generator. Not only does this model predict the way in which peak power varies but, using measured plasma flow conditions, the model can predict the magnitude of peak power with accuracy.

As a result of this research, the scientific feasibility of pulsed plasma MHD power generation has been established. Power levels and pulse energies have now been achieved for such applications as emergency communications, high energy lasers and high power microwave devices. Substantially higher performance levels are possible by size scaling within known hydrodynamic and electromagnetic scaling limits and by engineering improvements in the overall efficiency of the pulsed plasma MHD process. Multi-megajoule pulses at power levels of a few tenths of a terawatt are achievable while still retaining the features of a field portable, repetitively pulsed prime power source.

References

1. S.P. Gill, D.W. Baum, W.L. Shimmin, D. Mukherjee, "Explosive MHD Research," Artec Associates Inc. Final Report FR119, Office of Naval Research Contract N00014-75-C-0822, March 1977.
2. D.W. Baum, S.P. Gill, W.L. Shimmin, D. Mukherjee, "Research on Non-Ideal Plasma," Artec Associates Inc. Final Report FR126, Office of Naval Research Contract N00014-77-C-0463, May 1978.
3. D.W. Baum, S.P. Gill, R.F. Flagg, D. Mukherjee, J.D. Watson, "Shock Physics of Nonideal Plasmas," Artec Associates Inc. Annual Report AR130, Office of Naval Research Contract N00014-78-C-0354, 30 April 1979.
4. S.P. Gill, D. Mukherjee, "MHD Phenomena at High Magnetic Reynolds Number," Artec Associates Inc. Final Report FR137, Office of Naval Research Contract N00014-79-C-0565, December 1982.
5. D.W. Baum, J.D. Watson, S.P. Gill, W.L. Shimmin, "Dense Non-Ideal Plasma Research," Artec Associates Inc. Annual Report AR130, Office of Naval Research Contract N00014-78-C-0354, 30 April 1981.
6. Rogov, V.S., "Calculation of Plasma Conductivity," Tepl. Vys, Temp., 8, 1970, p. 689.
7. D. Mukherjee, "Nonideal Effects in Dense Argon and Xenon Plasmas,": Proceedings of First ONR Nonideal Plasma Workshop, Pasadena, California, 14-15 November 1978.
8. F.J. Rogers, Private Communication, Lawrence Livermore National Laboratory, December 1979.
9. F.J. Rogers, M. Ross, G.L. Haggin, L.K. Wong, "Equations of State for Self-Excited MHD Generator Studies," Lawrence Livermore Laboratory, UCID-18557, February 1980.

END

FILMED